A LETTERS JOURNAL EXPLORING THE FRONTIERS OF PHYSICS

Società Italiana di Fisica

sciences IOP Institute of Physics

Acoustic waves from mechanical impulses due to fluorescence resonant energy (Förster) transfer: Blowing a whistle with light

To cite this article: J. R. Zurita-Sánchez and C. Henkel 2012 *EPL* **97** 43002

View the article online for updates and enhancements.

Related content

- Topical Review
  Jan Willem Borst and Antonie J W G Visser
- Förster resonance energy transfer in a nanoscopic system on a dielectric interface
  Subrata Batabyal, Tanumoy Mondol, Kaustuv Das et al.
- Cold and ultracold molecules: science, technology and applications
  Lincoln D Carr, David DeMille, Roman V Krems et al.

Recent citations

- Trace formulas for nonequilibrium Casimir interactions, heat radiation, and heat transfer for arbitrary objects
  Matthias Krüger *et al*

This content was downloaded from IP address 200.23.5.162 on 26/10/2018 at 22:32

A Letters Journal Exploring the Frontiers of Physics

February 2012

EPL, **97** (2012) 43002
doi: 10.1209/0295-5075/97/43002

www.epljournal.org

Acoustic waves from mechanical impulses due to fluorescence resonant energy (Förster) transfer

Blowing a whistle with light

J. R. Zurita-Sánchez[1] and C. Henkel[2]

[1] *Instituto Nacional de Astrofísica, Óptica y Electrónica - Apdo. Postal 51 y 216, Puebla, Pue. 72000, Mexico*
[2] *Institut für Physik und Astronomie, Universität Potsdam - Karl-Liebknecht-Str. 24/25, 14476 Potsdam, Germany, EU*

received 27 October 2011; accepted in final form 11 January 2012
published online 21 February 2012

PACS 34.20.Gj – Intermolecular and atom-molecule potentials and forces
PACS 43.35.Ud – Thermoacoustics, high temperature acoustics, photoacoustic effect

Abstract – We present a momentum transfer mechanism mediated by electromagnetic fields that originates in a system of two nearby molecules: one excited (donor D^*) and the other in ground state (acceptor A). An intermolecular force related to fluorescence resonant energy or Förster transfer (FRET) arises in the unstable D^*A molecular system, which differs from the equilibrium van der Waals interaction. Due to the its finite lifetime, a *mechanical impulse* is imparted to the relative motion in the system. We analyze the FRET impulse when the molecules are embedded in free space and find that its magnitude can be much greater than the single recoil photon momentum, getting comparable with the thermal momentum (Maxwell-Boltzmann distribution) at room temperature. In addition, we propose that this FRET impulse can be exploited in the generation of acoustic waves inside a film containing layers of donor and acceptor molecules, when a picosecond laser pulse excites the donors. This acoustic transient is distinguishable from that produced by thermal stress due to laser absorption, and may therefore play a role in photoacoustic spectroscopy. The effect can be seen as *exciting a vibrating system like a string or organ pipe with light*; it may be used as an opto-mechanical transducer.

Copyright © EPLA, 2012

Introduction. – Electromagnetic fields can exert forces on an object that significantly influence its motion. These radiation forces have enabled the development of techniques for particle trapping or mechanical manipulation (optical tweezers) [1] and even the cooling of dilute atomic gases to extremely low temperatures [2]. One of these light forces originates from absorption in which the momentum carried by the field is transferred to the particle as mechanical momentum (radiation pressure).

In this paper, we focus on another momentum transfer mediated by electromagnetic fields that arises in a system of two molecules that are close to each other. When an excited molecule (donor) is nearby a ground-state molecule (acceptor), the electronic excitation can be swapped in a non-radiative way (fluorescence resonant energy or Förster transfer, FRET). During this process, an intermolecular force arises that differs from the equilibrium van der Waals interaction and is of larger range [3–5]. This force is an example of non-equilibrium dispersion interactions that have attracted quite some interest recently, both for microscopic [5–8] and macroscopic objects [9–11]. Since the initial state is unstable, this force $\mathbf{F}$ acts for a finite time τ that can be quite short compared to other mechanical scales. As a consequence, a mechanical impulse $\mathbf{P} = \mathbf{F}\tau$ is imparted to the relative motion of the donor-acceptor complex, while the electronic excitation is transferred. Our aim is to analyze the strength of this impulse as a function of the intermolecular separation and the donor and acceptor spectra. Since this momentum exchange occurs in the fluorescence resonant energy transfer, we call it the FRET *impulse*.

As an application, we study the FRET impulse between molecules embedded in a medium. The physics is related to the photoacoustic effect due to the thermal dilation of a medium in which molecules decay non-radiatively after excitation with light. Photoacoustic spectroscopy has been used to study biomolecular processes such as quantum yields of fluorescent proteins [12], protein folding [13], photosynthesis [14], and fluorophore-DNA binding [15]. The FRET impulse studied here provides an alternative

mechanism for generating acoustic waves. We consider layers of donor and acceptor molecules in an elastic film deposited on a substrate (fig. 2). A short light pulse, typically in the few-picosecond range, excites the donor molecules. The buildup of the FRET force between the donor and acceptor molecules is instantaneous on any mechanical time scale, after which it lasts for a few nanoseconds. As a consequence, it induces stress in the elastic material and generates acoustic waves. This sound can be as strong as in the conventional photoacoustic effect, but may be differentiated in the time and frequency domains.

This paper is organized as follows. We derive the FRET impulse when the molecules are embedded in a spatially inhomogeneous medium. This is followed by a detailed analysis for the case of free space. The next section is devoted to our proposal for generating acoustic waves from FRET. There the dynamics of these waves, including those due to heat deposited in the donor layer, is analyzed.

FRET impulse. – An excited donor molecule D^* is located at $\mathbf{r}_\mathrm{D}$, whereas an acceptor molecule A in the ground state is located at $\mathbf{r}_\mathrm{A}$. We consider that the molecules can be regarded as polarizable particles and describe the interaction between them classically. A similar approach for a bulk medium is followed by Cohen and Mukamel [7] who also showed the equivalence between the quantum and classical pictures. The interaction due to resonant energy transfer should not be confused with the eigenstates of the two-atom problem (even and odd superpositions $|D^*A\rangle \pm |DA^*\rangle$, bright and dark) whose potentials and decay rates show a very different distance dependence. The physics here is based on: i) distinguishable molecules and rapid dephasing of superposition states and ii) relatively short distances where the FRET rate dominates, although it is of fourth order in the dipole moments.

When the acceptor molecule interacts with an external electric field $\mathbf{E}(\mathbf{r},\omega)\,\mathrm{e}^{-\mathrm{i}\omega t} + \mathrm{c.c.}$ oscillating with angular frequency ω, the mean free energy $U(\mathbf{r}_\mathrm{A},\omega)$ of the molecule is modified as

$$U(\mathbf{r}_\mathrm{A},\omega) = -\mathrm{Re}[\mathbf{E}^*(\mathbf{r}_\mathrm{A},\omega)\cdot\boldsymbol{\mu}_\mathrm{A}(\omega)]. \tag{1}$$

Here, $\boldsymbol{\mu}_\mathrm{A}(\omega)$ is the absorption dipole of the acceptor and Re[...] denotes real part. If the absorption dipole is oriented along the (real) unit vector $\mathbf{n}_\mathrm{A}$, then $\boldsymbol{\mu}_\mathrm{A}(\omega) = \alpha_\mathrm{A}(\omega)\mathbf{n}_\mathrm{A}[\mathbf{n}_\mathrm{A}\cdot\mathbf{E}(\mathbf{r}_\mathrm{A},\omega)]$ with the polarizability $\alpha_\mathrm{A}(\omega)$. The aforementioned assumptions yield

$$U(\mathbf{r}_\mathrm{A},\omega) = -\mathrm{Re}[\alpha_\mathrm{A}(\omega)]|\mathbf{n}_\mathrm{A}\cdot\mathbf{E}(\mathbf{r}_\mathrm{A},\omega)|^2. \tag{2}$$

The acceptor molecule is driven by the electric field due to the emission dipole $\boldsymbol{\mu}_\mathrm{D}$ of the donor molecule, given by

$$\mathbf{E}(\mathbf{r},\omega) = \mathsf{G}(\mathbf{r},\mathbf{r}_\mathrm{D},\omega)\boldsymbol{\mu}_\mathrm{D}\sqrt{f_\mathrm{D}(\omega)}, \tag{3}$$

where $\mathsf{G}(\mathbf{r},\mathbf{r}',\omega)$ is the Green tensor for the medium where the donor and acceptor molecules are embedded, and the function $f_\mathrm{D}(\omega)$ gives the emission spectrum of the donor molecule, normalized to a unit integral over (positive) frequencies. We mention that on average, the donor's field is zero because the excited state D^* has no average dipole. But its dipole and field correlation functions are non-zero because of the excited state population, and this is what counts for the acceptor. Summing over all frequencies gives the total mean energy shift

$$\bar{U}(\mathbf{r}_\mathrm{A},\mathbf{r}_\mathrm{D}) = \int_0^\infty \mathrm{d}\omega\, U(\mathbf{r}_\mathrm{A},\mathbf{r}_\mathrm{D},\omega). \tag{4}$$

The FRET force exerted by the donor on the acceptor becomes

$$\mathbf{F}(\mathbf{r}_\mathrm{A},\mathbf{r}_\mathrm{D}) = -\nabla_{\mathbf{r}_\mathrm{A}}\bar{U}(\mathbf{r}_\mathrm{A},\mathbf{r}_\mathrm{D}). \tag{5}$$

This result is consistent with the non-equilibrium van der Waals-Casimir-Polder energy between two atoms derived in refs. [6,16]. It is worth noting that eq. (5) can have either sign, attractive or repulsive, depending on the detuning between the donor and acceptor spectra.

The initial state D^*A with the excited donor is not stable and decays along two pathways: $D^*A \to DA^* \to DA + h\nu_\mathrm{A}$: the donor molecule transfers its energy to the acceptor molecule (Förster energy transfer) and afterwards the acceptor molecule decays; and $D^* \to D + h\nu_\mathrm{D}$: the donor decays as if the acceptor molecule were absent. The total decay rate can therefore be written as $\gamma = \gamma_\mathrm{F} + \gamma_\mathrm{D}$. To obtain the Förster energy transfer rate γ_F, we divide the electromagnetic power spectrum that A absorbs from the donor, by the photon energy $\hbar\omega$. The absorbed power being proportional to $\omega\,\mathrm{Im}[\alpha_\mathrm{A}(\omega)]$, we get

$$\begin{aligned}\gamma_\mathrm{F}(\mathbf{r}_\mathrm{A},\mathbf{r}_\mathrm{D}) \;=\; & \frac{2}{\hbar}\int_0^\infty \mathrm{d}\omega\,\mathrm{Im}[\alpha_\mathrm{A}(\omega)]|\mu_\mathrm{D}|^2 f_\mathrm{D}(\omega) \\ & \times|\mathbf{n}_\mathrm{A}\cdot\mathsf{G}(\mathbf{r}_\mathrm{A},\mathbf{r}_\mathrm{D},\omega)\mathbf{n}_\mathrm{D}|^2,\end{aligned} \tag{6}$$

where the unit vector $\mathbf{n}_\mathrm{D}$ gives the orientation of the emission dipole, $\boldsymbol{\mu}_\mathrm{D} = \mu_\mathrm{D}\mathbf{n}_\mathrm{D}$. The decay rate of the donor molecule γ_D in the medium can be obtained from the local projected mode density [17]

$$\gamma_\mathrm{D}(\mathbf{r}_\mathrm{D}) = \frac{2}{\hbar}|\mu_\mathrm{D}|^2\,\mathrm{Im}[\mathbf{n}_\mathrm{D}\cdot\mathsf{G}(\mathbf{r}_\mathrm{D},\mathbf{r}_\mathrm{D},\omega_\mathrm{D})\mathbf{n}_\mathrm{D}], \tag{7}$$

where $\hbar\omega_\mathrm{D}$ is the electronic transition energy of the donor molecule, and we have assumed that the frequency dependence of the Green tensor is weak across the emission spectrum $f_\mathrm{D}(\omega)$. The total decay rate γ from eqs. (6), (7) is consistent with a calculation of the local mode density in the presence of the acceptor molecule [18]. We restrict our analysis to configurations where $\tau = 1/\gamma$ is short compared to mechanical response times. The FRET force thus imparts a momentum to the acceptor given (on average) by

$$\mathbf{P}(\mathbf{r}_\mathrm{A},\mathbf{r}_\mathrm{D}) = \tau(\mathbf{r}_\mathrm{A},\mathbf{r}_\mathrm{D})\mathbf{F}(\mathbf{r}_\mathrm{A},\mathbf{r}_\mathrm{D}), \tag{8}$$

and a momentum $-\mathbf{P}$ to the donor.

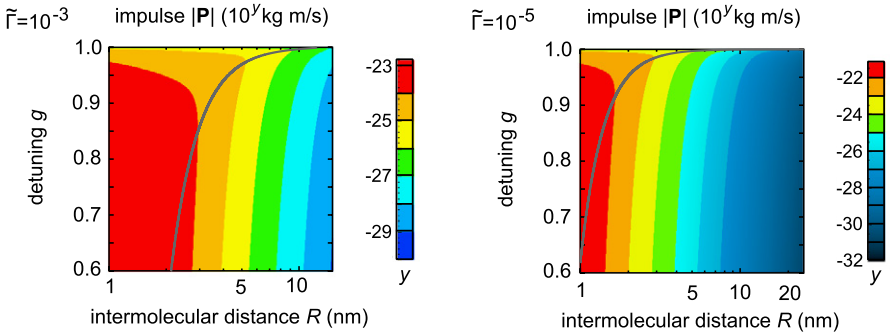

Fig. 1: (Colour on-line) FRET impulse *vs.* molecular distance R and detuning parameter $g=\omega_{\rm A}/\omega_{\rm D}$. We take the donor spectrum peaked at a free-space wavelength 628 nm ($\omega_{\rm D}=3\times10^{15}$ rad/s), an absorption dipole $\mu_{\rm A}=1.6\times10^{-29}$ Cm $=4.8$ D (electron charge times 1Å) and set $\Gamma_{\rm D}=\Gamma_{\rm A}\equiv\tilde{\Gamma}\omega_{\rm D}\ll\omega_{\rm D}$. The left (right) panel correspond to relatively wide (narrow) spectra. The gray lines illustrate the Förster radius (eq. (11)).

Case study: free space. – We analyze in more detail the case in which donor and acceptor are embedded in free space. Furthermore, we take the rotational average over the orientations of both dipole moments. The donor emission spectrum is assumed of Lorentzian shape

$$f_{\rm D}(\omega)=\frac{\Gamma_{\rm D}/\pi}{(\omega-\omega_{\rm D})^2+\Gamma_{\rm D}^2}, \tag{9}$$

whereas the acceptor polarizability is

$$\alpha_{\rm A}(\omega)=\frac{|\mu_{\rm A}|^2/\hbar}{\omega_{\rm A}-\omega-{\rm i}\Gamma_{\rm A}}. \tag{10}$$

Here, $\mu_{\rm A}$ is the matrix element of the absorption dipole, $\omega_{\rm D}$ and $\Gamma_{\rm D}$ ($\omega_{\rm A}$ and $\Gamma_{\rm A}$) are the central angular frequency and spectral width of the donor emission (acceptor polarizability), respectively. Since the typical Förster range is much smaller than the wavelength corresponding to $\omega_{\rm D,A}$, the quasi-static limit ($\omega_{\rm D,A}R/c\ll1$, $R=|\mathbf{r}_{\rm A}-\mathbf{r}_{\rm D}|$ is the intermolecular distance) applies.

By considering the aforementioned assumptions, the FRET impulse (eq. (8)) is oriented along the direction $\mathbf{n}_R$ joining the two molecules. The frequency integrals can be performed exactly with the method of residues, and we neglect a small non-resonant contribution. The decay rate becomes $1/\tau(R)=\gamma_{\rm D0}[1+(R_0/R)^6]$, where $\gamma_{\rm D0}$ is the free-space donor decay rate and the distance

$$R_0^6\approx\frac{\mu_{\rm A}^2c^3}{4\pi\varepsilon_0\hbar\omega_{\rm D}^3}\,\frac{\Gamma_{\rm A}+\Gamma_{\rm D}}{(\omega_{\rm A}-\omega_{\rm D})^2+(\Gamma_{\rm A}+\Gamma_{\rm D})^2} \tag{11}$$

may be identified with the Förster radius. Note, however, that the usual definition of the latter considers $\omega_{\rm D}=\omega_{\rm A}$ and also involves the non-radiative decay of D. For distances short enough for the decay rate $1/\tau$ to be dominated by the FRET process ($\gamma_{\rm F}\gg\gamma_{\rm D}$), we find

$$\mathbf{P}(R)\approx-\frac{3\hbar}{4R}\frac{\omega_{\rm A}-\omega_{\rm D}}{\Gamma_{\rm A}+\Gamma_{\rm D}}\mathbf{n}_R, \tag{12}$$

where the weak distance dependence is to be noted. In the opposite regime $\gamma_F\ll\gamma_{\rm D}$ (ε_0: vacuum permittivity),

$$\mathbf{P}(R)\approx-\frac{3\mu_{\rm A}^2c^3}{16\pi\varepsilon_0\omega_{\rm D}^3R^7}\,\frac{(\omega_{\rm A}-\omega_{\rm D})\,\mathbf{n}_R}{(\omega_{\rm A}-\omega_{\rm D})^2+(\Gamma_{\rm A}+\Gamma_{\rm D})^2} \tag{13}$$

featuring a typical dispersive lineshape as function of the detuning $\omega_{\rm A}-\omega_{\rm D}$ between the emission and absorption spectra. If the acceptor is red-shifted ($\omega_{\rm A}<\omega_{\rm D}$), the FRET interaction is repulsive.

These results are illustrated in fig. 1, where typical molecular parameters are considered (see caption). We take an emission spectrum peaked in the visible range and atomic-scale absorption and emission dipoles. At a given distance, there are two detunings $\pm(\omega_{\rm A}-\omega_{\rm D})_{\rm max}$ that give impulses with maximum modulus, as expected from the dispersive lineshape. At these optimal values, the distance is equal to the Förster radius R_0 (eq. (11)), shown as gray lines in fig. 1. The crossover from slow to fast decay with R as the distance crosses the Förster radius R_0 is also clearly visible in the plots.

Finally, we comment on the order of magnitude reached by the FRET impulse. The values one finds at short distance (see fig. 1) and with an optimal detuning are much larger than a single photon recoil $\hbar\omega_{\rm D}/c$ by a factor scaling as $(\lambda_{\rm D}/R)^4$. They are comparable to the typical momentum of a thermal Maxwell-Boltzmann distribution, $p_{\rm th}\approx8.3\times10^{-23}{\rm kg\,m/s}(M/10^3{\rm amu})^{1/2}(T/300\,{\rm K})^{1/2}$, where M is the molecular mass. If the molecules are bound together, the impulse will excite their relative (vibrational) motion. We discuss in the following section how this momentum kick relaxes when donor and acceptor molecules are embedded in a medium.

FRET and thermal acoustic waves. – We consider that two layers, one of donor molecules and the other of acceptor molecules, are embedded in an elastic film and deposited on a substrate, as depicted in fig. 2. The donor-acceptor separation R and the film thickness h can be controlled with nanometric precision by using the

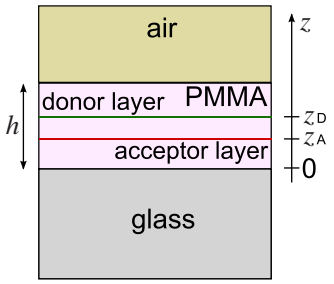

Fig. 2: (Colour on-line) Proposed experimental setup for detecting the FRET impulse. Two layers of donor and acceptor molecules are embedded in an elastic film. For definiteness, the calculations are done for a PMMA (polymethylmethacrylate) film on a glass substrate and exposed to air; the donor and acceptor layers are placed at $z_D = 10\,\text{nm}$ and $z_A = 7.5\,\text{nm}$.

Langmuir-Blodgett technique. The donor layer is excited by a laser pulse in a frequency band where film and acceptor molecules cannot absorb light. This creates a FRET force between excited donor molecules and the acceptor molecules, on the one hand, this force becoming a source of acoustic waves. On the other hand, if the donor molecules have intrinsic losses, part of the absorbed energy is transformed into heat which subsequently diffuses in the film. The thermal dilation and the time-dependent temperature gradient causes elastic stress, which also generates acoustic waves. The question arises as to whether the two acoustic signals are distinguished in the time and frequency domains. We therefore solve the acoustic wave equation

$$\frac{1}{\tilde{c}^2}\frac{\partial^2 u}{\partial t^2} - \frac{\partial^2 u}{\partial z^2} = q_F(z,t) + q_H(z,t). \tag{14}$$

Here, u is the displacement, $\tilde{c}$ is the speed of sound in the film, and q_F and q_H are the FRET and thermal acoustic sources, respectively. Hereafter we assume that the excitation pulse is much shorter ($\sim 1\,\text{ps}$) than the transients of u and neglect the momentum transfer from absorption (of the order of the photon recoil).

The FRET force is modeled as a localized stress with exponential decay over the time scale τ. Its strength is proportional to the impulse P_F per D^*A pair and the area density of excited donors. Therefore (for $t \geqslant 0$)

$$q_F(z,t) = \frac{P_F n_{D^*}}{\tau B}\exp(-t/\tau)\left[\delta(z-z_D) - \delta(z-z_A)\right], \tag{15}$$

where $\delta(\ldots)$ is the Dirac-δ function, z_D (z_A) is the donor (acceptor) layer position, and the other symbols are explained in table 1. The parameters there yield a dimensionless prefactor $P_F n_{D^*}/(\tau B) \approx -0.008$ ($\tau = 3.3\,\text{ps}$) in eq. (15), the sign indicating an attractive FRET force. We also checked that the interfaces and films have sufficiently similar electromagnetic impedances, so that the FRET force does not significantly differ from its expression in a homogeneous medium.

Table 1: Symbols and parameter values for acousto-elastic parameters in the system of fig. 2.

Parameter		Value
Film thickness	h	$20\,\text{nm}$
Excited donor density	n_{D^*}	$4\,\text{nm}^{-2}$
FRET impulse/pair	P_F	$-2\times10^{-23}\,\text{kg m/s}$
D^*A complex lifetime	τ	3.3–333 ps
Sound speed*	$\tilde{c}$	$1.591\,\text{nm/ps}$
Bulk elastic modulus*	B	$3\,\text{GPa}$
Pulse energy/area	$\mathcal{E}/A$	$1\,\text{nJ}/100\,\mu\text{m}^2$
Transmittance	$\mathcal{T}(z_D)$	0.96
Heat conversion	e_H	0.001
Density*	ρ	$1.185\,\text{g/cm}^3$
Heat capacity*	c_p	$1.466\,\text{J/K g}$
Thermal diffusivity**	α	11–$1100\,\text{nm}^2/\text{ns}$
Dilation coefficient*	β	$7\times10^{-5}\,\text{K}^{-1}$

*The parameter value corresponds to PMMA.
**The typical diffusion coefficient for PMMA is $\alpha = 110\,\text{nm}^2/\text{ns}$.

To estimate the thermal stress $q_H(z,t)$, we solve for the temperature distribution created by absorption and subsequent thermal diffusion. The absorbed energy density is localized in the donor layer (see table 1) and is given by

$$W(z) = e_H\frac{\mathcal{T}(z_D)\mathcal{E}}{A}\delta(z-z_D). \tag{16}$$

The heat capacity of the film relates this to the instantaneous temperature change in the donor layer, $\Delta T = W(z)/(\rho c_p)$. Consequently, the diffusion equation for the temperature distribution $T(z,t)$ becomes [19]

$$\frac{\partial T}{\partial t} = \alpha\frac{\partial^2 T}{\partial z^2} + S\delta(t)\delta(z-z_D), \tag{17}$$

where the source amplitude is $S = e_H\mathcal{T}(z_D)\mathcal{E}/(\rho c_p A) \approx 5.5\,\text{K nm}$ for the parameters given in table 1. The increase in temperature dilates the material, giving rise to thermal stress proportional to the temperature gradient. The thermal source for the acoustic field is therefore

$$q_H(z,t) = -3\beta\frac{\partial T}{\partial z}. \tag{18}$$

The largest temperature gradients occur inside the film for short enough times after the laser pulse. We are therefore justified in using the solution to the diffusion equation (eq. (17)) for an unbounded medium, that is,

$$T(z,t) = \frac{S}{\sqrt{4\pi\alpha t}}\exp[-(z-z_D)^2/(4\alpha t)], \quad t \geqslant 0. \tag{19}$$

Combined with eq. (18), this formula provides the thermal acoustic source in eq. (14).

We solve the wave equation (14) using Green functions. This leads to an explicit expression for the displacement field $u(z,t)$ in the PMMA film, including partial reflections

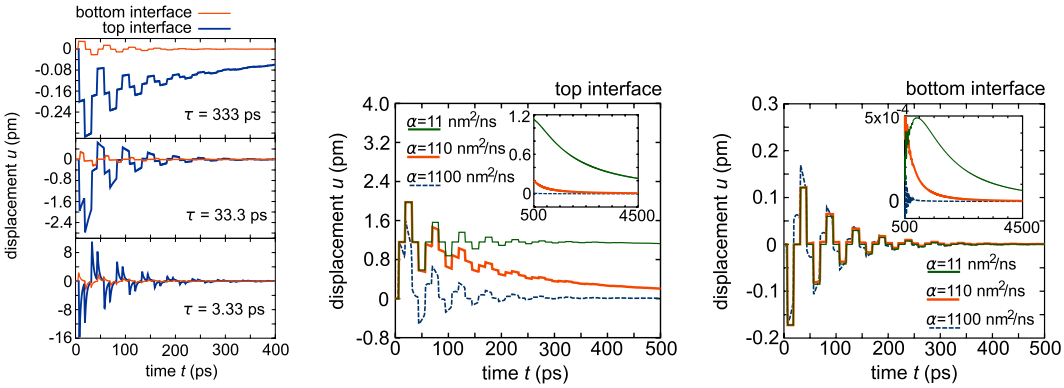

Fig. 3: (Colour on-line) Left: FRET acoustic waves. The displacement $u_{\rm F}(z,t)$ for the top interface (PMMA-air, $z=20\,$nm) and bottom interface (PMMA-glass, $z=0\,$nm) as a function of time. The lifetime of the D^*A complex is taken as $\tau=330\,$ps, $\tau=33.3\,$ps, and $\tau=3.33\,$ps. The donor (acceptor) layer is at $z_{\rm D}=10\,$nm ($z_{\rm A}=7.5\,$nm). Middle and right: thermal acoustic waves. The displacement $u_{\rm H}(z,t)$ as a function of time for a thermal diffusion constant $\alpha=11\,{\rm nm}^2/{\rm ns}$, $110\,{\rm nm}^2/{\rm ns}$, and $1100\,{\rm nm}^2/{\rm ns}$, and for $z=20\,$nm (top interface) and $z=0\,$nm (bottom interface). The insets show the long-time evolution of the displacement.

at its top and bottom interfaces. The displacement is, obviously, a sum of two contributions of the form

$$u_{\rm F}(z,t) = \frac{\tilde{c}P_{\rm F}n_{\rm D^*}}{B}\sum_{n=0}^{\infty}a_n\{[1-{\rm e}^{-\tilde{t}_{{\rm D}n}/\tau}]\theta(\tilde{t}_{{\rm D}n}) -[1-{\rm e}^{-\tilde{t}_{{\rm A}n}/\tau}]\theta(\tilde{t}_{{\rm A}n})\}, \quad (20)$$

$$u_{\rm H}(z,t) = \frac{3\tilde{c}\beta S}{4\alpha}\int_0^h {\rm d}z_1\sum_{n=0}^{\infty}a_n\frac{z_1-z_{\rm D}}{|z_1-z_{\rm D}|} \times{\rm erfc}\left[|z_1-z_{\rm D}|/\sqrt{4\alpha\tilde{t}_{1n}}\right]\theta(\tilde{t}_{1n}). \quad (21)$$

The complementary error function is denoted as erfc[...] and $\theta(t)$ is the unit step function. The dimensionless amplitudes a_n involve the acoustic reflection coefficients at the interfaces and become smaller as n increases. The delayed times $\tilde{t}_{k\,n}(z,z_k,t)$ ($k={\rm D},{\rm A},1$) correspond to the arrival of acoustic rays at the observation point z at time t from the source point z_k, after multiple round trips between the film boundaries.

The acoustic waves generated by the two types of sources are illustrated in fig. 3. The distance between the donor and acceptor layers is taken as $R=|z_{\rm D}-z_{\rm A}|=2.5\,$nm. For simplicity, we keep the FRET impulse per pair $P_{\rm F}$ constant and vary the FRET lifetime τ. This would correspond to properly chosen molecular parameters. The displacements at the top and bottom interfaces are plotted in fig. 3, and may be observed with differential reflectance spectroscopy [19,20]. One observes a rapid contraction of the film, followed by the "ringdown" of the acoustic waves as they bounce back and forth in the film. Note the abrupt slope changes at certain instants resulting from the multiple reflections (roundtrip time $2\,h/\tilde{c}\approx 25\,$ps). As the FRET impulse gets shorter, the oscillation amplitude becomes higher (see fig. 3). This can be explained by the higher force (stress) in eq. (15). Figure 3 also shows that the transient oscillations are larger at the PMMA-air interface than at the PMMA-glass interface. This is a consequence of the disparity between the two reflection coefficients. The impedance mismatch at the bottom and top interfaces leads to reflection amplitudes -0.703 and 0.9996 for the sound waves there, respectively: indeed, the acoustic impedances of PMMA and glass are comparable, while for air it is very small. The spectrum of this acoustic transient is shown in fig. 4(a) and discussed below.

In fig. 3, we also plot the transient sound due to thermal stress, for different values of the thermal diffusion constant α. For the pulse parameters of table 1, the FRET and thermal stresses give roughly the same order of magnitude of elastic displacement. This can be changed by adjusting the energy and absorption cross-section of the incoming pulse, of course. The typical time scale for sound from thermal stress is of the order of the diffusion time $\tau_{\rm H}\sim h^2/\alpha\approx 360\,$ps–36 ns, determined by the diffusivity α of the film. This effect is illustrated in the insets of fig. 3: the larger α, the shorter the transient. Also we notice from fig. 3 that the sound pattern immediately after the excitation pulse is nearly independent of α, although the shapes of the curves differ notoriously. Similar to the acoustic waves due to FRET attraction, the displacement amplitude is larger at the interface with the higher reflection coefficient (PMMA-air), as is seen from the comparison of the middle and right plots of fig. 3.

The normalized spectra of the FRET (thermal) displacements $|\tilde{u}_{\rm F(H)}(h,\nu)|^2$ at the top surface are depicted in fig. 4. Sharp peaks occur at the frequencies $\nu_m=m\nu_0$ ($m=1,3,5,\ldots$, $\nu_0=\tilde{c}/(4h)$), which are the resonant frequencies of an acoustic tube with one end open and the other closed (organ pipe). This is as expected from the acoustic reflection amplitudes given above. The peaks in the FRET sound spectrum decrease as the lifetime τ increases, except for the zero-frequency component which is independent of τ (see fig. 4(a)). The thermal spectrum follows the opposite behavior: the spectrum is practically independent of the thermal diffusivity α with the exception of the low-frequency

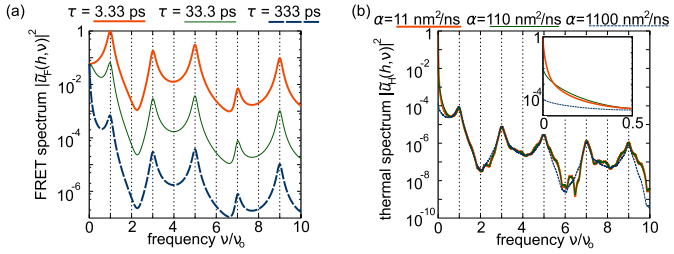

Fig. 4: (Colour on-line) (a) Normalized acoustic power spectrum due to FRET compression, $|u_F(h,\nu)|^2$, evaluated at the top surface. Three different lifetimes τ as shown. (b) Normalized power spectrum due to thermal stress, $|u_H(h,\nu)|^2$, at the top surface. Three values for the thermal diffusivity α as shown. Inset: spectrum at low frequencies. Each figure is normalized with respect to the maximum value of three data series. Here $\nu_0 = \tilde{c}/(4h) = 19.9\,\mathrm{GHz}$.

range in which the zero-frequency component decreases as α increases (see fig. 4(b)). Therefore, the FRET and thermal sound exhibit distinguishable spectral features.

Conclusions. – We have provided a transparent derivation of the non-equilibrium radiative force between an excited (donor D^*) and a ground-state (acceptor A) molecule. The finite lifetime of D^* leads to a mechanical momentum that excites the relative motion of the D^*A complex. Its magnitude can be quite significant and its sign depends on the frequency mismatch between the emission and absorption spectra.

We have considered a simple photoacoustic setup with a donor layer and an acceptor layer embedded in an elastic film. An incoming short laser pulse selectively excites the donor layer and initiates elastic stress between donor and acceptor molecules that lasts over the duration of the FRET process. This stress acts as a temporal source of acoustic waves that can be measured from the displacements of the film interfaces, using optical reflectance in a pump-probe technique [19,20]. The sound waves ring down as they leave into the substrate after multiple reflections, similar to a piano string after it has been struck, albeit on a time scale of a few hundred picoseconds. We have shown that the conventional photoacoustic effect (thermal dilation due to non-radiative losses) generates sound waves whose spectra and amplitude scaling can be differentiated from the "FRET sound". In particular, the duration of this wave source is governed by thermal diffusion in the film, whereas its amplitude can be controlled by modifying the energy and cross-section of the incident pulse. The FRET sound therefore provides a donor-acceptor specific opto-mechanical transducer that may enlarge the current capabilities of photoacoustic spectroscopy in the study of biological processes (*e.g.*, protein folding).

It would be interesting to extend this analysis to the FRET force that acts after the first impulse, once the acceptor molecule is excited: since the detuning of the spectra is reversed, the pair DA^* gets an impulse of opposite sign. There are good reasons, however, for the impulses to have different magnitudes: the emission spectrum is shifted, donor and acceptor lifetimes differ, and the absorption and emission dipoles may have different orientations, even on the same molecule.

* * *

JRZ-S acknowledges the support provided by SEP-CONACyT through the Basic Science Grant CB-2008/98449-F. CH thanks M. Bargheer, H. Haakh, D. Neher, and S. Volz for stimulating discussions.

REFERENCES

[1] Ashkin A. and Dziedzic J. M., *Appl. Phys. Lett.*, **28** (1976) 333.
[2] Cohen-Tannoudji C., *Atomic motion in laser light,* in *Fundamental Systems in Quantum Optics*, edited by Dalibard J., Raimond J. M. and Zinn-Justin J., *Lecture Notes from Les Houches School of Physics, Session LIII, 1990* (Elsevier, Amsterdam) 1992, pp. 1–164.
[3] Niemax K., *Phys. Rev. Lett.*, **55** (1985) 56.
[4] Power E. A. and Thirunamachandran T., *Chem. Phys.*, **198** (1995) 5.
[5] Sherkunov Y., *Phys. Rev. A*, **75** (2007) 012705.
[6] Power E. A. and Thirunamachandran T., *Phys. Rev. A*, **51** (1995) 3660.
[7] Cohen A. E. and Mukamel S., *Phys. Rev. Lett.*, **91** (2003) 233202; *J. Phys. Chem. A*, **107** (2003) 3633.
[8] Tomas M.-S., *J. Phys. A*, **41** (2008) 164020.
[9] Henkel C., Joulain K., Mulet J.-P. and Greffet J.-J., *J. Opt. A: Pure Appl. Opt.*, **4** (2002) S109.
[10] Krüger M., Emig T., Bimonte G. and Kardar M., *EPL*, **95** (2011) 21002.
[11] Messina R. and Antezza M., *EPL*, **95** (2011) 61002.
[12] Kurian E., Predergast F. G. and Small J. R., *Biophys. J.*, **73** (1997) 466.
[13] Abbruzzetti S., Crema E., Masino L., Vecli A., Viappiani C., Small J. R., Libertini L. J. and Small E. W., *Biophys. J.*, **78** (2000) 405.
[14] Herbert S. K., Han T. and Vogelmann T. C., *Photosynth. Res.*, **66** (2000) 13.
[15] Bugs M. R. and Cornélio M. L., *Eur. Biophys. J.*, **31** (2002) 232.
[16] Sherkunov Y., *Phys. Rev. A*, **79** (2009) 032101.
[17] Novotny L. and Hecht B., *Principles of Nano-Optics*, 1st edition (Cambridge University Press, Cambridge) 2006.
[18] Carminati R., Greffet J.-J., Henkel C. and Vigoureux J. M., *Opt. Commun.*, **261** (2006) 368.
[19] Perrin B., *Investigation of short-time heat transfer effects by an optical pump-probe method*, in *Microscale and Nanoscale Heat Transfer*, edited by Volz S., *Top. Appl. Phys.*, Vol. **107** (Springer, Heidelberg, Berlin) 2007, Chapt. 13, pp. 333–59.
[20] Richardson C. J. K., Ehrlich M. J. and Wagner J. W., *J. Opt. Soc. Am. B*, **16** (1999) 1007.